Nanoscale

Plasmonic effect of spray deposited Au nanoparticles on the performance of inverted organic solar cell

Journal:	*Nanoscale*
Manuscript ID:	NR-ART-06-2014-003270.R1
Article Type:	Paper
Date Submitted by the Author:	03-Jul-2014
Complete List of Authors:	Chaturvedi, Neha; Indian Institute of Technology Delhi, Center for Energy Studies Swami , Sanjay; Indian Institute of Technology Delhi, Center for Energy Studies Dutta, Viresh; Indian Institute of Technology Delhi, Center for Energy Studies

Plasmonic effect of spray deposited Au nanoparticles on the performance of inverted organic solar cell

Neha Chaturvedi[a1], Sanjay Kumar Swami[a] and Viresh Dutta[a]

[a]Photovoltaic Laboratory, Centre for Energy Studies, Indian Institute of Technology Delhi, New Delhi-110016, India

Abstract

Gold nanoparticles with varying sizes were prepared by the spray process under an electric field (DC voltages of 0 V and 1kV applied to the nozzle) for studying their role in inverted organic solar cells (ITO/Au/ZnO/P3HT: PCBM/Ag) . The application of electric field during spray process resulted in a smaller size (35nm as compared to 70nm without the electric field) of the nanoparticles with more uniform distribution. This gave rise to a difference in the surface plasmon resonance (SPR) effect created by the gold nanoparticles (Au NPs), which then affected the solar cell performance. The photovoltaic performances of plasmonic inverted organic solar cells (ITO/Au/ZnO/P3HT: PCBM/Ag) using spray deposited Au and ZnO layers (both at 1kV) showed an improved efficiency. A fast exciton quenching in P3HT:PCBM layer was obtained by using spray deposited Au layer in between ITO and ZnO layer . The absorption spectra and internal power conversion efficiency (IPCE) curve showed that the Au nanoparticles provide significant plasmonic broadband light absorption enhancement which resulted in the enhancement of J_{SC} value. A maximum efficiency of 3.6% was achieved for the inverted organic solar cell (IOSC) with an exceptionally high short circuit current density of ~ 15 mA/cm^2 which is due to the additional photon absorption and the corresponding increase seen in IPCE spectrum. The spray technique can be easily applied for the direct formation of Au nanoparticles in fabrication of IOSC with improved performance over a large area.

Keywords: Au nanoparticles, Localised surface plasmon resonance, Spray process, Electric field and Plasmonic solar cell.

[1] Corresponding author at: Centre for Energy Studies, Indian Institute of Technology Delhi, New Delhi 110016. India. Tel. +9111-2659-6489; fax. +9111-2659-1261.
E-mail address: nchaturvedi9@gmail.com

Introduction

Organic solar cells have attracted considerable attention due to their light weight, cost effectiveness and solution processibility.[1-8] The inherent drawback of short lifetime in the conventional device structure (ITO/PEDOT:PSS/P3HT:PCBM/Al) due to the acidic nature of PEDOT:PSS and low work function of Al electrode has led to the research towards inverted organic solar cell(IOSC). [9-11] In IOSC the charge collecting nature of the electrodes is reversed giving it a more stable structure of ITO/ZnO/P3HT:PCBM/Ag. ZnO is known as a good electron transport layer used in organic solar cells.[12-14] Plasmonic effects in solar cells have been explored due to the increased light absorption in the polymer film from the scattering or near field enhancement caused by the metallic nanoparticles. When these nanoparticles are irradiated by light, a localized enhanced electric field initiating from the localized surface plasmon resonance (LSPR) is generated all around the metallic nanoparticles.[15-17] This LSPR plays an important role in improving the device performance by enhancing the light absorption in active layer and hence the photoelectric conversion efficiency of organic solar cell. [18-20] In plasmonic solar cells the metal nanoparticles (Ag or Au) can be incorporated in the carrier transport layer, in to the active layer, on top of the active layer (P3HT:PCBM) or in between the carrier transport layer and active layer. [21-26] LSPR effect in thin film solar cells depends on different shape and distribution of nanoparticles (NPs). [27, 28]There are many reported methods to exploit the LSPR effect either in inorganic solar cell or in organic solar cell to improve the power conversion efficiency (PCE). [29-32] Since the efficiency of organic solar cell is mainly limited by the absorption of photons in the wavelength range close to the HUMO-LUMO gap of the organic layer (and the subsequent collection of charges at the electrodes), an enhancement in the absorption region using LSPR effect of metal NPs can play an important role in improving the photovoltaic parameters.

There are many reported methods for fabricating the Au NPs films from the pre-synthesized colloidal Au NPs (with or without ligands) such as sol gel, in situ preparation, immersion, atomic layer deposition (ALD), plasma assisted physical vapour deposition (PAPVD) etc. [33-35] There are also reports on direct formation of Au NPs on glass substrate using ultrasonic spray technique and spray pyrolysis technique. [36, 37] We have used the spray technique due to its inherent advantages of low cost, large area coverage, easy thickness control, less material wastage and ease in tunability of the deposited nanoparticles size. To the best of our knowledge we are reporting for the first time the use of electric field for size variation in the

spray formed Au NPs on ITO substrate for application in the plasmonic IOSC(ITO/Au/ZnO/P3HT:PCBM/Ag).The electron transport layer (ZnO) is also deposited by the same technique. Thus, the reported technique of direct formation of Au NPs eliminates the requirement of NPs formation separately and will reduce complete device fabrication time. The effect of electric field on the optical and structural properties of the deposited Au nanoparticle films and their role on the IOSC performance are presented in the paper.

Experimental

The spray deposition set-up is described in detail in our earlier publication. [38] The spray solution for Au NPs formation is prepared by taking 0.3mM auric acid (Molychem) in DI water and sonicate this solution for 5 min. Nitrogen gas is used as a carrier gas. The optimized deposition parameters are: substrate temperature-350℃, solution flow rate - 1ml/min and nozzle to substrate distance - 18cm. The electric field is created by connecting a DC power supply (up to 1kV) between the nozzle and a circular electrode placed 4mm below the nozzle. The spray solution recipe and spray deposition parameters for electron transport layer (ZnO) on the Au layer are described in our earlier publication. [39]

The spray deposited films are characterized using ZEISS EVO -50 model scanning electron microscope for surface morphological study, Bruker Dimension Icon atomic force microscope (AFM) in tapping mode to know the roughness and Perkin Elmer Lambda 1050 UV–Vis–NIR spectrophotometer for optical absorption studies. X-ray diffraction (XRD) studies were done using an X-ray diffractometer (Phillips X'PERT PRO), having CuKα incident beam (λ=1.54 Å). Dektak XT surface profiler was used to measure the thickness of the deposited films. The photoluminescence (PL) spectra were recorded using a Perkin-Elmer luminescence spectrometer (model: LS-55) having a xenon flash lamp as the source of excitation at excitation wavelength of 470nm. For the time-resolved PL (TRPL) measurements the samples were excited using 475 nm pulsed laser and the transient signal was recorded using a time correlated single photon counting (TCSPC) spectrometer (PMA-C 192-N-M, Picoquant).

For the fabrication of plasmonic IOSC we first cleaned the ITO substrate by using sonication steps in soap solution, DI water, acetone and isopropyl alcohol for 15min each. The film of Au nanoparticles with a thickness of ~ 5nm was deposited using spray process on the cleaned ITO substrate. ZnO film with a thickness of ~ 30nm was spray deposited on the Au film. A blend of regioregular Poly(3-hexylthiophene) (P3HT) and [6,6]- Phenyl C_{61}-butyric acid methyl ester

(PCBM) (both from Sigma Aldrich) dissolved in 1-2 dichlorobenzene, with a weight ratio of 1:0.8 was used for the active layer deposition. The blend layer with a thickness of ~150 nm was spin coated (in air) on spray deposited ZnO layer. The deposited active layer was annealed at 140°C for 15min.The Ag electrode (100nm) was deposited by using thermal evaporation method at 1.0×10^{-5} Torr to obtain an effective device area of 0.09 cm^2. J–V characteristics of these devices were measured under AM 1.5 G illumination using an Oriel Sol 3A, a class AAA solar simulator, with a Keithley 2440 source meter. The simulator was calibrated using an NREL certified Si solar cell. Internal power conversion efficiency (IPCE) spectra of these devices were recorded at room temperature using SpeQuest quantum efficiency measurement system from RERA solutions, Netherlands.

Results and discussion

Morphological properties

Scanning electron microscopy (SEM) image in Fig. 1(a) clearly shows the formation of Au nanoparticles by spraying of the auric acid solution. The nanoparticles are randomly distributed with average particle size of 70nm. The shape of the spray deposited nanoparticles is not uniform over the surface and there is also some agglomeration. On applying the DC voltage (1kV) during the spray process the deposited nanoparticles are uniformly distributed with a reduced average size of 30nm (Fig. 1(b)). The size reduction and uniformity of Au nanoparticles are as expected because on applying the DC voltage the electrostatically charged spray droplets will become finer with a more uniform size distribution.

The surface morphology of spray deposited ZnO layer on the Au layer is shown in Fig. 2. The large size spray deposited Au nanoparticles with the applied voltage = 0 V are projecting out of the thin ZnO layer (Fig. 2(a)). On the other hand, there is full coverage of smaller Au nanoparticles deposited with the applied voltage =1kV by the ZnO film (Fig. 2(b)). All characteristics of spray deposited ZnO layer on ITO substrate are already reported in our previous publication. [39] The role of the size of Au nanoparticles and the coverage by ZnO layer on the photovoltaic parameters of IOSC s will be discussed later.

The electric field effect on the surface morphology and roughness of spray deposited layers are seen in the two dimensional (2D) as well as three dimensional (3D) AFM topography images shown in Fig. 3. These AFM images are taken at the scale of 5μm×5μm. The root mean square

roughness ($R_{r.m.s}$) of spray deposited ZnO layer on Au NP layer is 24nm which gets reduced to 10nm on applying the voltage during the spray deposition of Au as well as ZnO layers due to the formation of finer droplets after applying DC voltage. These finer droplets spread in corona cone giving rise to smooth surface morphology over large area. As can be seen from AFM images that the large sized Au NPs are projecting out of the spray deposited ZnO layer which is leading to a higher roughness. These large size NPs (70nm) will penetrate into the active layer used in the formation of plasmonic inverted solar cell. The reduced roughness for the smaller nanoparticles is expected to enhance the IOSC performanec by giving a better pathway to deposit polymer layer as well as the SPR effect in the active layer as will be discussed later.

Structural properties

The XRD spectra of spray deposited Au nanoparticles is shown in Fig. 4. The well-defined peak positions and their orientations positions are well matched with the JCPDS card no. 089-3697. The crystallinity of spray deposited Au layer is getting enhanced on applying the voltage resulting in an increased peak intensity. A good crystalline film should provide a better charge transport and extraction for improving PCE of the device.

Optical properties

The normalized absorption spectra of spray deposited Au nanoparticle film are shown in Fig. 5. The SPR peak of spray deposited Au layer (0V) is at $\boldsymbol{\lambda}_{max}$ ~ 570nm with SPR bandwidth (FWHM) of 100nm and gets blue shifted towards $\boldsymbol{\lambda}_{max}$ ~ 533 nm with SPR bandwidth of 50nm on applying the voltage. These absorption peaks are well matched with the absorption peaks of the P3HT:PCBM film. The creation of finer droplets under the electric field is the reason for the change in the SPR band position and the reduction in FWHM. By creating a different electric field during the spray deposition one can change the size and distribution of NPs and accordingly tune the SPR band very easily.[37] To confirm the contribution of the LSPR effects for both the spray deposited Au nanoparticles films, we measured the absorption spectra of spin coated P3HT layer deposited on the top of ITO/Au/ZnO structure (Fig. 6). For reference the absorption spectra of spin coated P3HT layer on top of spray deposited ZnO layers (0V and 1kV) without the Au NPs layer (only ITO/ZnO) is also taken.

From the absorption spectra it can be seen that the absorption for P3HT deposited on ITO/Au(70nm)/ZnO is higher and extended up to 1000 nm than that for the reference device(ITO/ZnO (0V and 1kV)) which is having an absorption up to 690nm only. The absorption gets further enhanced till 1200nm for the P3HT deposited on electric field assisted spray deposited Au NPs as well as ZnO layer (ITO/Au (35nm)/ZnO). This increase is attributed to the LSPRs of Au NPs (size ~70 nm) that penetrate in to the active layer and Au NPs (size ~35 nm) that touch the active layer. The absorption enhancement from 400nm to 660nm (absorption range of P3HT) will fully contribute in the improvement of device performance.

The further enhancement in the range of 690nm -1200nm may not play major role in improving our device performance. But if it is applied for OPV devices fabricated using active blend layer with spectrally extended absorption range from 700nm-1200 nm, there can be a significant improvement in the performance. There are reports that for large size nanoparticles the back scattering power dominates the forward scattering and this reduces the absorption in the active layer. [40] The LSPR effect depends on the shape, distribution as well as the separation distance between the nanoparticles. The spray deposited Au nanoparticles (0V) have an irregular shape with agglomerated large sized NPs of random distribution (Fig. 1(a)), therefore the contribution of LSPR effect in absorption enhancement is less due to the back scattering effect. While due to the reduced size and uniform distribution for the electric field assisted spray deposited Au NPs, the contribution of LSPR effect in absorption enhancement is higher.

Role of the spray deposited Au nanoparticles on photovoltaic performance

To find out the role of spray deposited Au nanoparticles two sets of devices were prepared: **Device D1** (ITO/ZnO/P3HT:PCBM/Ag) and **Device D2** (ITO/Au/ZnO/P3HT:PCBM/Ag). To further study the role of electric field on spray deposited Au layer two more sets of devices were prepared by applying DC voltage (1kV) during the spray deposition of Au layer as well as ZnO layer: **Device D3** (ITO/ZnO/P3HT:PCBM/Ag) and **Device D4 (**ITO/Au/ZnO/P3HT:PCBM/Ag).

The J-V characteristics of plasmonic IOSC (ITO/Au/ZnO/P3HT:PCBM/Ag) and IOSC (ITO/ZnO/P3HT:PCBM/Ag) are shown in Fig.7. Device D1 shows the power conversion efficiency of 2.3%. On introducing the spray deposited Au nanoparticle (70nm) layer between

ITO and spray deposited ZnO layer (device D2) the power conversion efficiency increases to 2.9% with improved J_{SC} and FF values of 13.8mA/cm^2 and 39.0%, respectively (Table. 1).

Table. 1. Photovoltaic parameters of IOSCs.

Device Name	J_{SC}(mA/cm^2)	V_{OC}(V)	FF (%)	η (%)
Device D1	11.8	0.54	36.5	2.3
Device D2	13.8	0.54	39.0	2.9
Device D3	13.1	0.54	37.9	2.6
Device D4	15.6	0.56	41.5	3.6

The device D4 using both the electric field assisted spray deposited small Au nanoparticles (35nm) layer and ZnO layer shows the highest efficiency of 3.6% with remarkable increment in J_{SC} value (15.6 mA/cm^2) which is mainly due to the LSPR effect of Au NPs enhancing the absorption in the active layer. An improvement is also seen in the V_{OC} and FF values which increases from 0.54V to 0.56V and from 37.9% to 41.5% , respectively in comparison to device D3 (PCE=2.6%). The increment in Voc and FF values are due to the improved film qualities by applying electric field during deposition as discussed before.

The role of LSPR effect in enhancing the absorption is seen from the IPCE spectra (Fig. 8) which show the same trend of increment in J_{SC} values for all the four IOSCs. Expectedly the highest IPCE of 75% is obtained for the best device D4 proving the effectiveness of the LSPR effect due to small size of the nanoparticles. The IPCE for the larger sized nanoparticles (70 nm) is of course lesser. The small difference in the IPCE of the IOSCs using different ZnO layers can be attributed to the improvement in the ZnO layer prepared under the electric field. Thus, the combined effect of the LSPR due to small sized Au nanoparticles and improved ZnO layer properties is causing the improved performance in device D4. The large size Au nanoparticles

(70nm) used in device D2 will project beyond the 30nm ZnO layer and penetrate the P3HT:PCBM layer leading to reduced D/A interface area. [41] This can also cause a difference in the IPCE spectra.

Effect of spray deposited different size Au NPs on the Photoluminescence spectra

As described above there is variation in photovoltaic parameters of plasmonic IOSC by using different sizes of spray deposited Au NPs. To further investigate these results and to know the LSPR effect on the exciton generation rate we performed the photoluminescence (PL) measurement. As the main contributor of light absorption and exciton generation in active layer is the donor phase (P3HT), therefore we measured the PL spectra of spin coated P3HT film on ITO/Au/ZnO film with different spray deposited Au NPs (Fig. 9).

There is an enhancement in the PL intensity after using spray deposited layer of Au NPs in between ITO and ZnO layer. This enhancement is due to the fact that an increment in the degree of light absorption as well as light excitation rate occurs due to the LSPR excitation. [15] From PL spectra we see that upon excitation of the LSPR there is an enhancement in light absorption and the number of photo generated excitons in P3HT. Due to this the PL intensity gets enhanced in comparison to P3HT spin coated on ZnO without Au layer. This increment is higher on using the electric field assisted spray deposited Au NPs than that for spray deposited Au NPs with the applied voltage = 0V. This difference is because the PL intensity mainly depends on the changes in the light absorption, affecting the light excitation rate and exciton quenching at metal/organic interfaces. For spray deposited Au NPs (applied voltage = 1kV) there is an enhancement in the absorption of P3HT film as compared to that for the spray deposited Au NPs with the applied voltage = 0V (Fig. 6) which contributes to the enhancement of PL intensity. As the spray deposited large size Au NPs (70nm) will penetrate the 30nm ZnO layer and enter in to P3HT layer, there is quenching at metal/organic interface giving lower PL intensity. While the spray deposited small size Au NPs (35nm) will reach till the interface of P3HT layer giving a higher PL intensity with a high exciton generation rate. This enhanced exciton generation rate will help in producing more J_{SC} and increased PCE.

Time Resolved Photolumniscence: Effect of Au NPs on exciton quenching

Time resolved PL measurements (Fig.10) are performed to understand the coupling process between the plasmonic field and the photogenrated excitons within the active blend

layer. TRPL provides the information about the influence of the plasmonic effect on the photophysical process between the donor and acceptor phases and hence the role of different NPs sizes in terms of exciton lifetime (τ).The average exciton lifetime ($\tau_{exciton}$) is calculated using the following equation:

$$\tau_{exciton} = (A_1\tau_1^2 + A_2\tau_2^2)/(A_1\tau_1 + A_2\tau_2)$$

where τ_1 and τ_2 are the two lifetime values with corresponding amplitudes of A_1 and A_2 for a given transient curve.

For the spin coated P3HT:PCBM film on spray deposited ZnO layer (ITO/ZnO/P3HT:PCBM) the values of two fitted exponential constants τ_1 and τ_2 are 34ns and 2.90ns, respectively: providing a corresponding exciton lifetime of 25ns. After using the spray deposited Au layer between ITO and ZnO layer (ITO/Au/ZnO/P3HT:PCBM) the values of two exponential constants τ_1 and τ_2 are 26ns and 2.24ns respectively, providing $\tau_{exciton}$ value as 20ns. By using the spray deposited Au and ZnO layers under the effect of electric field (ITO/Au/ZnO/P3HT:PCBM) the values of τ_1 and τ_2 are 15ns and 1.70ns, respectively with $\tau_{exciton}$ = 9ns.These results suggest that by using spray deposited Au layer between ITO and ZnO layer the excitons are getting quenched faster in comparison to that without the Au layer. Further, the excitons get quenched much faster on using electric field assisted spray deposited Au and ZnO layers (ITO/Au/ZnO/P3HT:PCBM). The use of spray deposited Au layer (with NP size of 35 nm) results in a greater absorption of light with enhanced exciton generation; however, when these excitons reach to P3HT:PCBM interface, the degree of charge carrier dissociation is also increased. This fast exciton dissociation plays an important role in improving the device performance.

Conclusions

Direct formation of different sizes of Au nanoparticles on ITO substrate achieved using the spray process. This allows for the preparation of Au nanoparticles formation directly on ITO substrate for the plasmonic IOSC fabrication without including any post-deposition treatment. Uniform, smooth, well distributed and crystalline Au nanoparticles are deposited by applying a DC voltage during spray process. The UV-Vis absorption range and exciton generation rate of polymer are enhanced due to LSPR effect of Au nanoparticles. The fast exciton quenching is achieved by using electric field assisted spray deposited Au and ZnO layers in between ITO and P3HT:PCBM film. There are 17% and 26% increment in the J_{SC} and PCE values of IOSC

(Device D2) using spray deposited Au nanoparticle (70nm) layer in between ITO substrate and ZnO layer in comparison to IOSC (Device D1) without including Au layer. Using electric field (applied voltage =1kV) assisted spray deposited Au nanoparticles (35nm) and ZnO layers (Device D4) the J_{SC} and PCE show increments of 32% and 56% ,respectively in comparison to IOSC(Device D1). LSPR effect of Au nanoparticles in giving rise to these differences is clearly established and the role of the size difference for spray deposited layers with applied voltage = 0 V and 1 kV has been demonstrated. The possibility of large area deposition as well as roll to roll deposition makes this spray technique suitable for plasmonic IOSC.

Acknowledgment

The work reported in this paper was done under the Department of Science and Technology project **"Advancing the efficiency and production potential of excitonic solar cells".** One of the author S.K.S acknowledge the financial support from Ministry of New and Renewable Energy (MNRE), New Delhi. The authors gratefully acknowledge the fruitful discussions with Dr. V. K. Komarala on Plasmonics as well as Transient PL measurement and Mr. Nikhil Chander on Plasmonics. Authors would like to thanks Dr. A. F. Khan for helping in Transient PL measurement. The authors would also like to thank Miss Shilpi Chaudhary's contributions in initiating the spray deposition of polymer layers.

References

1 M. Yu, Y. Z. Long, B. Sun and Z. Y. Fan, *Nanoscale*, 2012, **4**, 2783-2796.

2 S. Gunes, H. N. Neugebauer and S. Sariciftci, *Chem. Rev.*, 2007**, 107**, 1324–1338.

3 L.J. Pegg, S. Schumann and R.A. Hatton, *ACS Nano*, 2010, **4**, 5671-5678.

4 J.G. Xue, B.P. Rand, S. Uchida and S.R. Forrest, *Adv. Mater.*, 2005, **17**, 66–71.

5 P. Poudel and Q. Q. Qiao, *Nanoscale*, 2012, **4**, 2826-2838.

6 W.L. Ma, C.Y. Yang, X. Gong, K. Lee and A.J. Heeger, *Adv. Funct. Mater.*, 2005, **15**, 1617–1622.

7 G. Dennler, C. Lungenschmied, H. Neugebauer, N.S. Sariciftci and A. Labouret, *J. Mater. Res.*, 2005, **20**, 3224–3233.

8 F. Yang and S.R. Forrest, *ACS Nano*, 2008, **2**, 1022–1032.

9 P. Qin, G. Fang, N. Sun, X. Fan, Q. Zheng, F. Cheng, J. Wan and X. Zhao, *Thin Solid Films*, 2012, **520**, 3118-3124.

10 R.L.Z. Hoye, D.M. Rojas, D.C. Iza, K.P. Musselman and J.L.M. Driscoll, *Sol. Energy Mater. Sol. Cells*., 2013, **116**, 197–202.

11 M. S. White, D. C. Olson, S. E. Shaheen, N. Kopidakis and D. S. Ginley, *Appl. Phys. Lett.*, 2006, **89**, 143517-1–143517-3.

12 V. Kumar, N. Singh, V. Kumar, L. P. Purohit, A. Kapoor, O .M. Ntwaeaborwa and H .C. Swart, *J. Appl. Phys.*, 2013, **114**, 134506-1 – 134506-6.

13 V. Kumar, H .C. Swart, O .M. Ntwaeaborwa, R. E. Kroon, J. J. Terblans, S. K. K. Shaat, A. Yousif and M. M. Duvenhage, *Mater. Lett.,* 2013, **101**, 57-60.

14 V. Kumar, N. Singh, R. M. Mehra, A. Kapoor, L. P. Purohit and H. C. Swart, *Thin Solid Films*, 2013, **539**, 161-165.

15 J. L. Wu, F.C. Chen, Y.S. Hsiao, F.C. Chien, P. Chen, C.H. Kuo, M.H. Huang and C.S. Hsu, *ACS Nano*, 2011, **5**, 959–967.

16 L. Qiao, D. Wang, L. Zuo, Y. Ye, J. Qian, H. Chen and S. He, *Appl. Energy*, 2011, **88**, 848–852.

17 S.W. Baek, G. Park, J. Noh, C. Cho, C.H. Lee, M.K. Seo, H. Song and J.Y. Lee, *ACS Nano,* 2014, **8**, 3302-3312.

18 A. J. Morfa, K. L. Rowlen, T. H. Reilly, M.J. Romero and J. V. Lagemaat, *Appl. Phys. Lett.*, 2008, **92**, 013504-1-013504-3.

19 T. Matsumoto, T. Oku and T. Akiyama, *Jpn. J. Appl. Phys*., 2013, **52**, 04CR13-1- 04CR13-5.

20 C. M. Liu, C. M. Chen, Y. W. Su, S. M. Wang and K. H. Wei, *Org. Electron*., 2013, **14**, 2476–2483.

21 L. Lu, Z. Luo, T. Xu and L. Yu, *Nano Lett*., 2013, **13**, 59-64.

22 J. Yang, J. You, C. Chen, W.C. Hsu, H. Tan, X.W. Zhang, Z. Hong and Y. Yang, *ACS Nano*, 2011, **5**, 6210-6217.

23 K. Liu, Y. Bi, S. Qu, F. Tan, D. Chi, S. Lu, Y. Li, Y. Kou and Z. Wang, *Nanoscale*, 2014, **6**, 6180-6186.

24 A. Kirkeminde, M. Retsch, Q. Wang, G. Xu, R. Hui, J. Wu and S.Ren, *Nanoscale*, 2012, **4**, 4421-4425.

25 F.X. Xie, W.C.H. Choy, C.C.D. Wang, W.E.I. Sha and D.D.S. Fung, *Appl. Phys. Lett.*, 2011**, 99**, 153304-1-153304-3.

26 J.N. Pei, J.L. Tao, Y.H. Zhou, Q.F. Dong, Z.Y. Liu, Z.F. Li, F.P. Chen, J.B. Zhang, W.Q. Xu and W. J. Tian, *Sol. Energy Mater. Sol. Cells.*, 2011, **95**, 3281–3286.

27 H.S. Noh, E.H. Cho, H.M. Kim, Y.D. Han and J. Jinsoo, *Org. Electron.*, 2013, **14**, 278–285.

28 K. Islam, A. Alnuaimi, E. Battal, A. K. Okyay and A. Nayfeh, *Sol. Energy*, 2014, **103**, 263–268.

29 M. G. Kang, T. Xu, H. J. Park, X. Luo and L. J. Guo, *Adv. Mater*., 2010, **22**, 4378–4383.

30 S. S. Kim, S. I. Na, J. Jo, D. Y. Kim and Y. C. Nah, *Appl. Phys. Lett.*, 2008, **93**, 073307.

31 A. P. Kulkarni, K. M. Noone, K. Munechika, S. R. Guyer and D. S. Ginger, *Nano Lett*., 2010, **10**, 1501–1505.

32 R. J. Zhou, Y. Zheng, L.Qian, Y. X. Yang, P.H. Holloway and J. G. Xue, *Nanoscale*, 2012, **4**, 3507-3514.

33 V. Kumar and H. Wang, *Org. Elect.*, 2013, **14**, 560–568.

34 J. Schmitt, P. Machtle, D. Eck, H. Mohwald and C. A. Helm, *Langmuir*, 1999, **15**, 3256-3266.

35 L. Amelao, D. Barreca, G. Bottaro, A. Gasparotto, E. Tondello, M. Ferroni and S. Polizzi, *Appr. Chem. Mater.*, 2004, **16**, 3331-3338.

36 M. D. L. Garza, I. López and I. Gómez, *Adv. in Mater. Science and Eng*. 2013, **2013**, 1-5.

37 N. Kumar, V. K. Komarala and V. Dutta, *Phys. Status Solidi RRL.*, 2012, **6**, 9-10.

38 N. Chaturvedi, F. Alam, S. K. Swami and V. Dutta, *J. Appl. Phys.*, 2013, **114**, 184501-1-184501-6.

39 N. Chaturvedi, S. K. Swami, A. Kumar and V. Dutta, *Sol. Energy Mater. Sol. Cells*, 2014, **126**, 74–82.

40 S. W. Baek, J. Noh, C.H. Lee, B. S. Kim, M. K. Seo and J. Y. Lee, *Scient. Reports.* 2013, **3**, 1726-1732.

41 X. Chen, L. Zuo, W. Fu, Q. Yan, C. Fan, and H. Chen, *Sol. Energy Mater. Sol. Cells,* 2013, **111**, 1–8.

List of Figures:

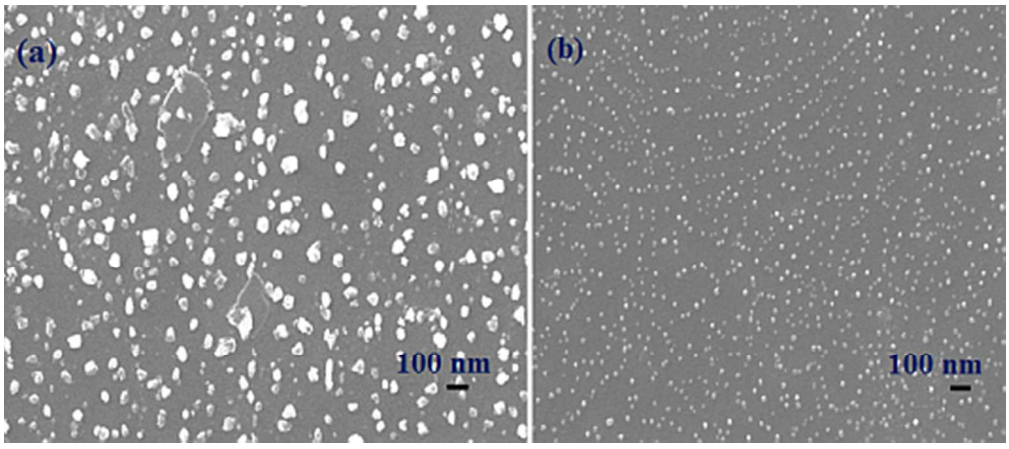

SEM images of spray deposited Au nanoparticles at (a) 0V (b) 1kV.
44x19mm (300 x 300 DPI)

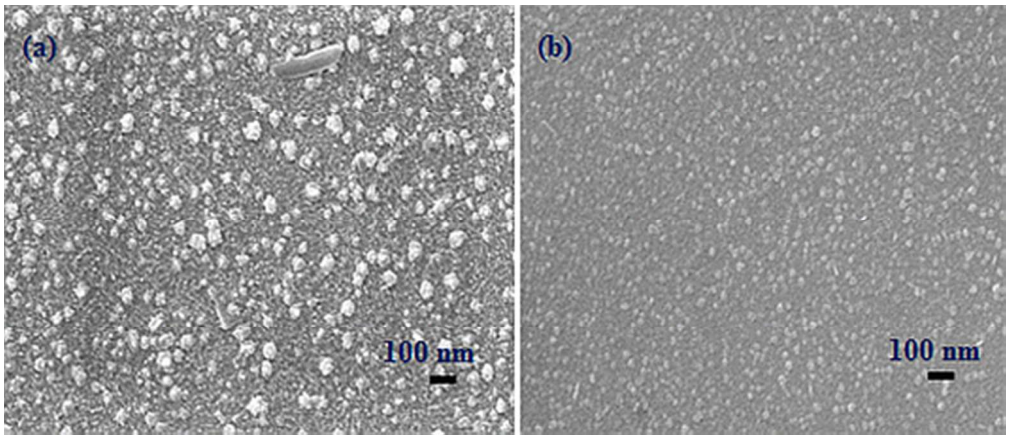

SEM images of spray deposited ZnO layer on Au nanoparticles at (a) 0V (b) 1kV.
44x19mm (300 x 300 DPI)

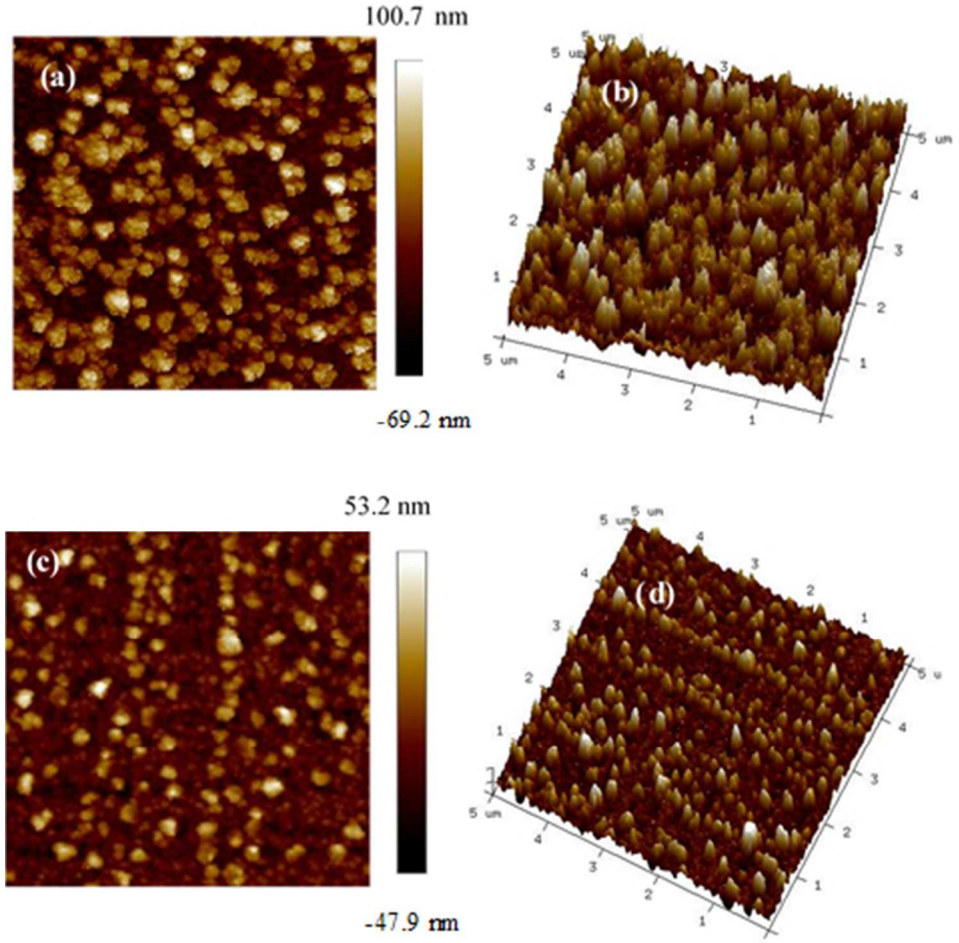

AFM images of spray deposited ZnO layer on Au nanoparticles at (a) 0V 2D image (b) 0V 3D image (c) 1kV 2D image (d) 1kV 3D image.
40x41mm (300 x 300 DPI)

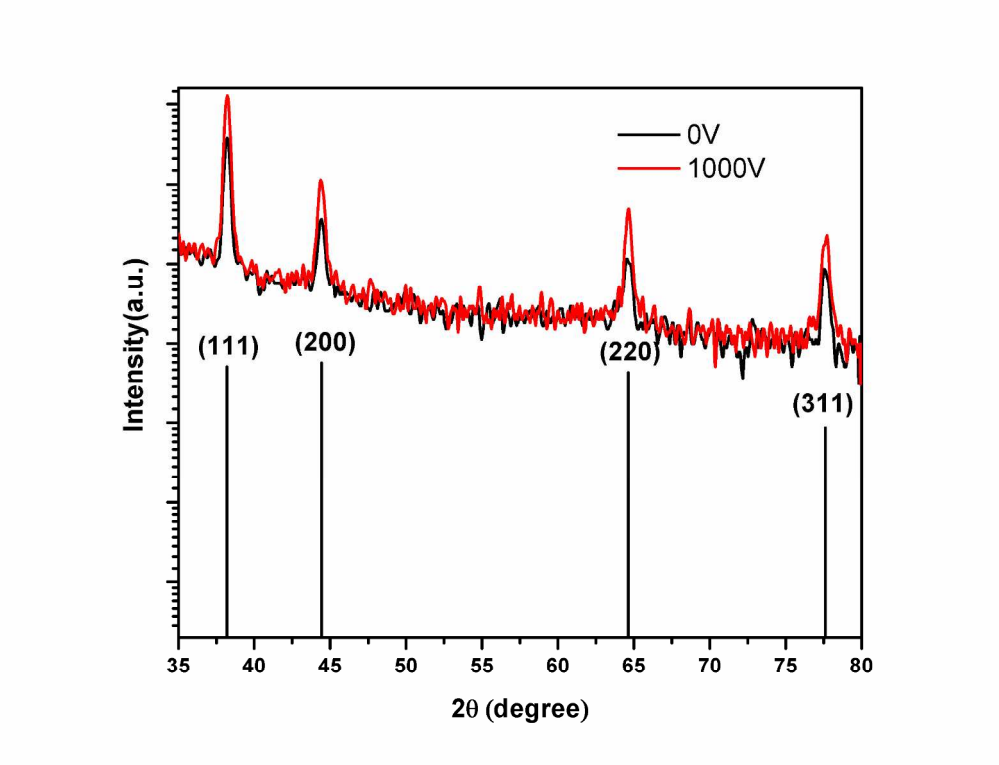

XRD spectra of spray deposited Au layer with applied voltage = 0V and 1kV.
259x198mm (300 x 300 DPI)

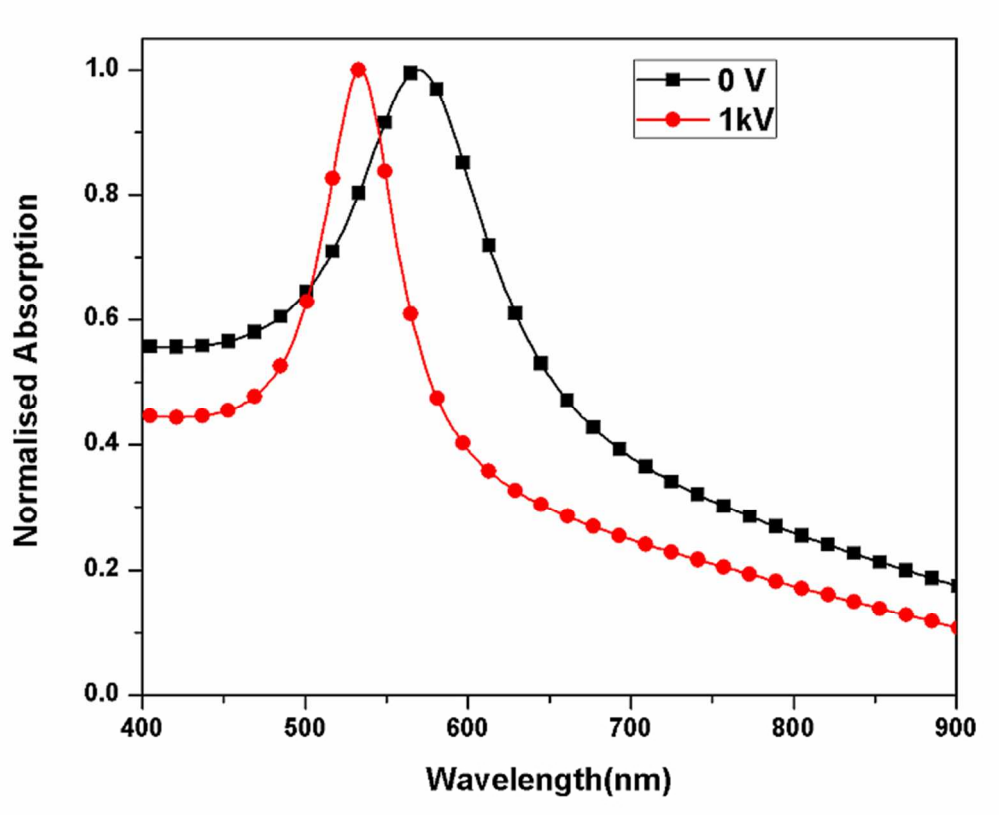

UV-Vis absorption spectra of spray deposited Au nanoparticles layer showing the shift due to the applied voltage.
61x50mm (300 x 300 DPI)

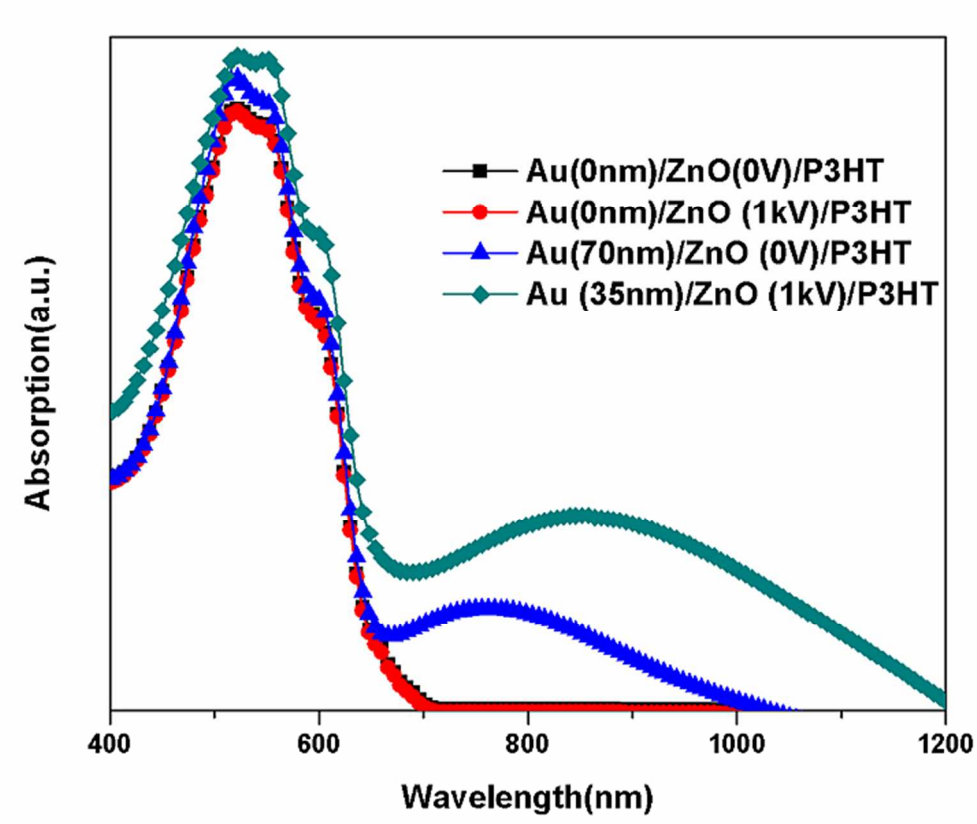

UV-Vis absorption spectra of spin coated P3HT layer on ITO/Au/ZnO structure.
61x51mm (300 x 300 DPI)

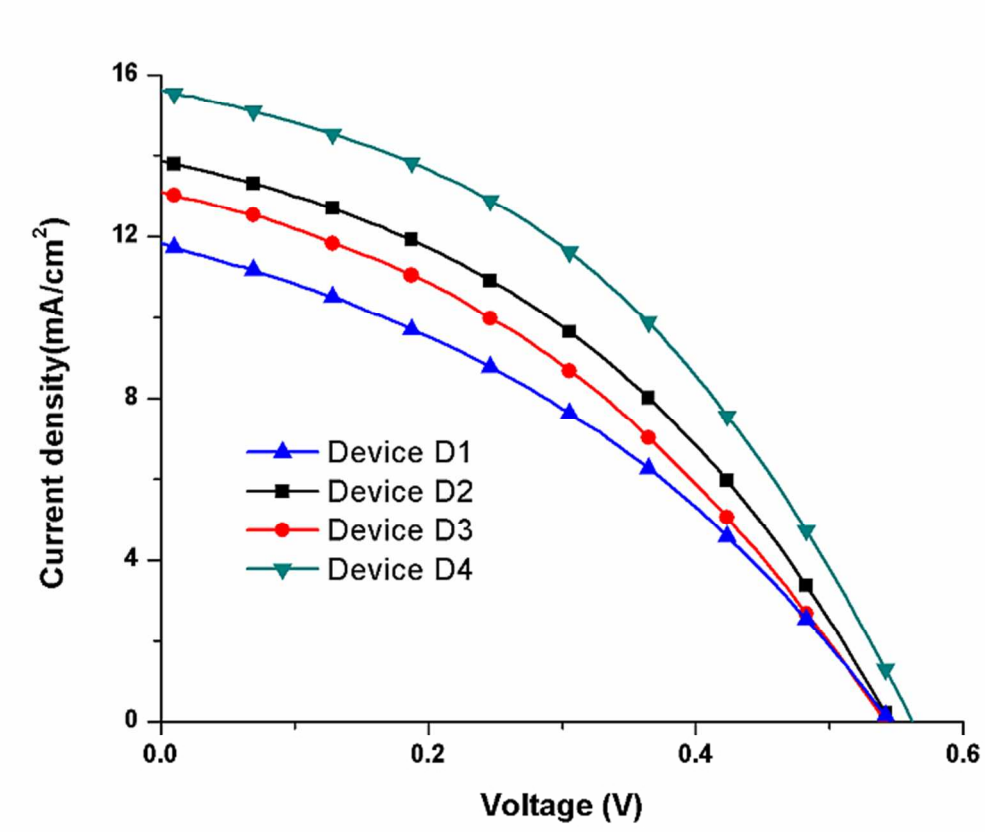

J-V characteristics of IOSCs with and without the Au nanoparticle layers.
61x52mm (300 x 300 DPI)

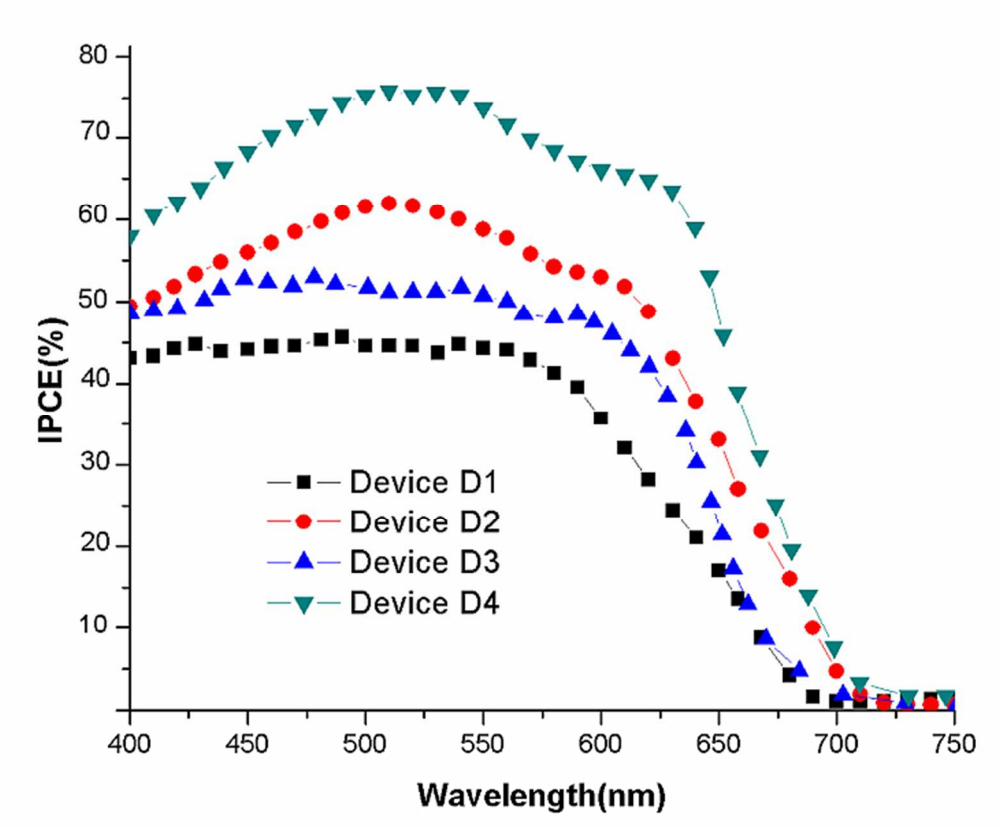

IPCE spectra of IOSC devices.
61x51mm (300 x 300 DPI)

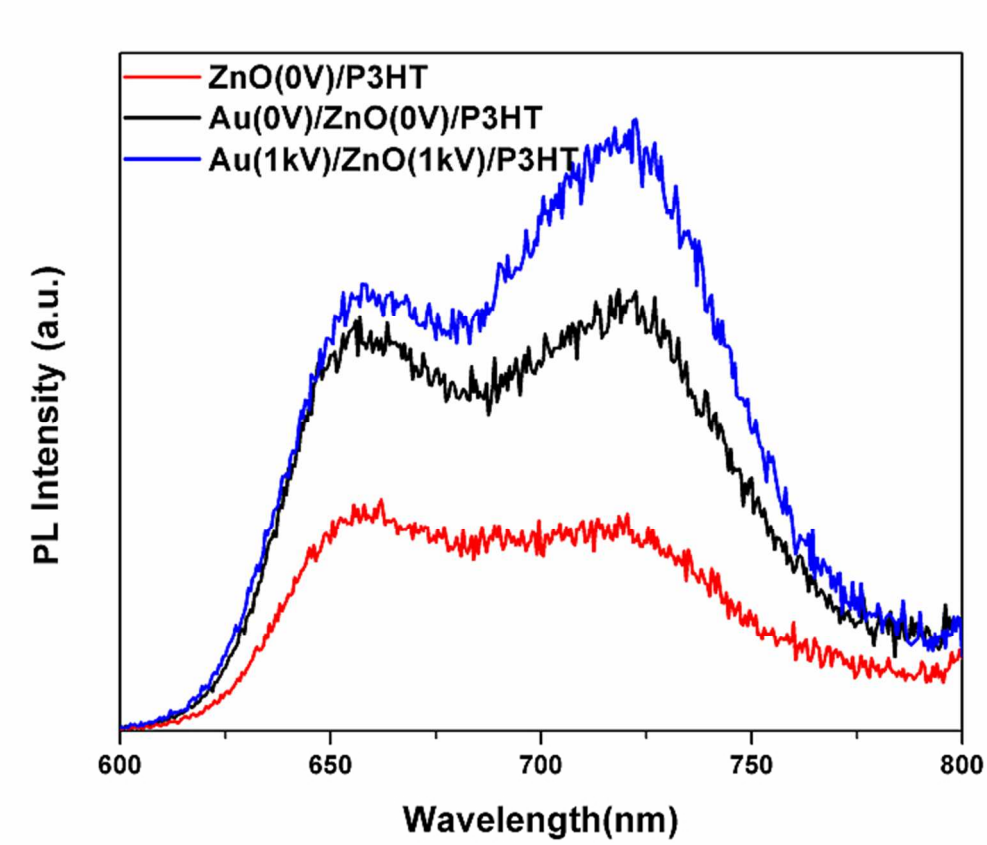

PL spectra of spin coated P3HT layer on different structures.
60x51mm (300 x 300 DPI)

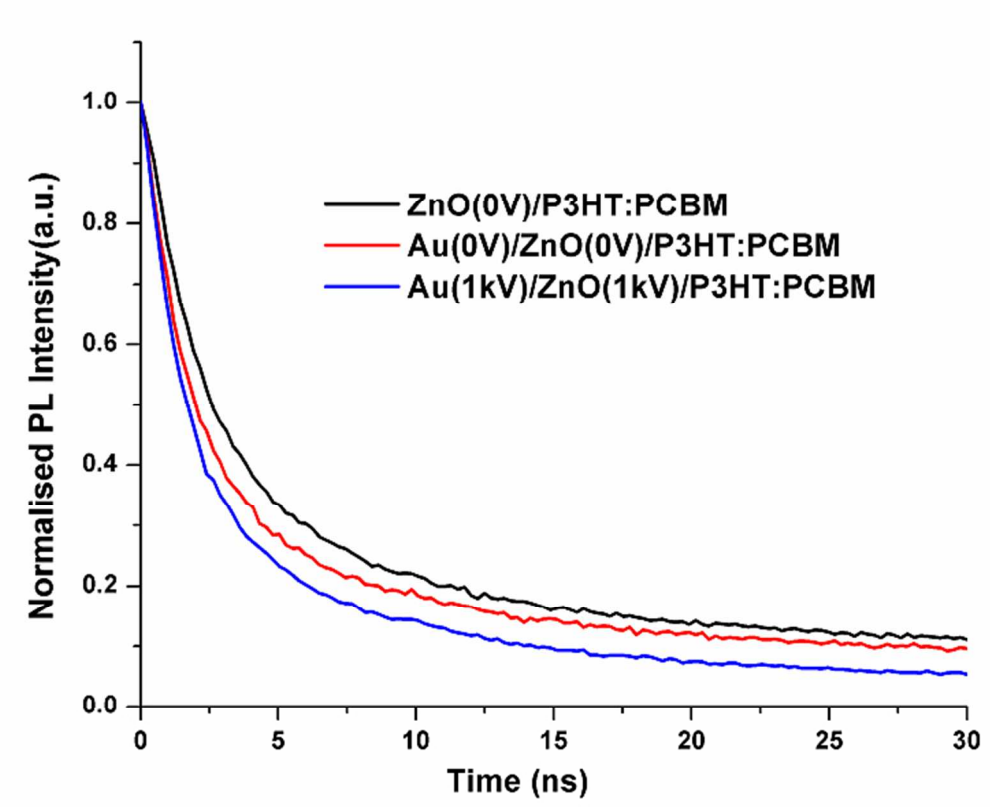

Time-resolved PL spectra of P3HT: PCBM layer spin coated on different structures.
61x50mm (300 x 300 DPI)